

# Studying thermal effects of laser on tissue using implicit finite volume method

M. Esfand Abadi\*, M. H. Miran Baygi\*, A. Mahloojifar\* and S. Moghimi\*

**Abstract:** In this paper, thermal effects of laser irradiance on biological tissue is investigated using computer simulations. Earlier attempts in this field made use of finite difference and finite element techniques. Here a novel approach is adopted to improve the results. The effect of our implicit approach on the convergence procedure and accuracy of results, with different timing steps, is explored. Monte Carlo method is used in combination with the finite volume algorithm in order to obtain a profile of light distribution and heat transport in tissue. It is shown that implicit finite volume technique has not only acceptable accuracy, but also high stability for different timing steps.

**Keywords:** Laser, Simulation, Monte Carlo method, Implicit finite volume, Convergence.

## 1 Introduction

In last three decades, laser has found a variety of applications. It was first used in eye surgeries for therapeutic purposes. Later it became an attractive choice in different fields of medicine. Nowadays, noninvasive surgeries are achieved using various laser systems.

During irradiation of the tissue by laser, different types of interaction may occur, among which thermal effects have a larger contribution. Therefore, modeling this effect enables us to predict the optimal laser wavelength, pulse width, and irradiance power. Also, it helps us to predict the outcome of the surgery, which is very desirable as it facilitates the process of treatment. In fact laser parameters and tissue characteristics dominate the process of laser tissue interaction. Optical behavior of tissue has a strong dependency on laser wavelength, while heat transportation is merely directed by tissue thermal characteristics [1]. Heat transport process is defined by a differential equation which needs to be solved numerically. In order to solve these equations, which describe dynamic systems, different techniques have been adopted. Finite volume, which was defined based on finite difference method, was first introduced by *Borris* and *Brook* in 1973 [1]. In this paper implicit finite volume method is used to solve heat transport equation, as it shows higher stability criteria than those used formerly [2, 3, 4].

In the following sections, the interaction of diode laser with dog and human prostate tissue along with the effect of timing steps in achieving the final temperature in different tissue layers is investigated using the techniques mentioned above. The results will show that implicit finite volume method can be used as a reliable and accurate technique in simulation of heat distribution within homogeneous and heterogeneous tissues.

## 2 Modeling light distribution

Monte Carlo method is used for simulation of light distribution in the target tissue [5]. The most significant advantage of this method is that it can be applied to the actual tissue geometries because of its high flexibility. Various quantities such as light absorption and heat generation rate can be calculated using two and three dimensional simulation of the interaction process. Figure 1 illustrates a flowchart for the variable step size Monte Carlo method [5,6,7,8].

Optical characteristics of the target tissue, such as absorption and scattering coefficients, have been used as the input to the simulation program. As the photon travels a specific distance, defined by the simulator, it may be scattered, absorbed, propagated undisturbed, internally reflected, or transmitted out of the tissue. The photon is repeatedly moved until it either escapes from or is absorbed by the tissue. If the photon escapes from the tissue, the reflection or transmission of the photon is recorded. If the photon is absorbed, the position of the absorption is recorded. This process is repeated until the desired number of photons has been used in running the program. The recorded absorption and escaping profiles will approach true values (for a tissue with the specified optical properties) as the number of photons propagated approaches infinity. By simulating the propagation of N

Iranian Journal of Electrical & Electronic Engineering, 2005.

Paper first received 16th January 2006 and in revised form 27th November 2006.

\* The authors are with the Department of Electrical Engineering, Tarbiat Modares University, Tehran, Iran.

E-mail: [m\\_shams@modares.ac.ir](mailto:m_shams@modares.ac.ir), [mh\\_miranbaygi@yahoo.com](mailto:mh_miranbaygi@yahoo.com), [mahlooji@modares.ac.ir](mailto:mahlooji@modares.ac.ir), [moghimi@modares.ac.ir](mailto:moghimi@modares.ac.ir).

photons, the absorption matrix is obtained, which will be used later to calculate the heat distribution profile in the target tissue.

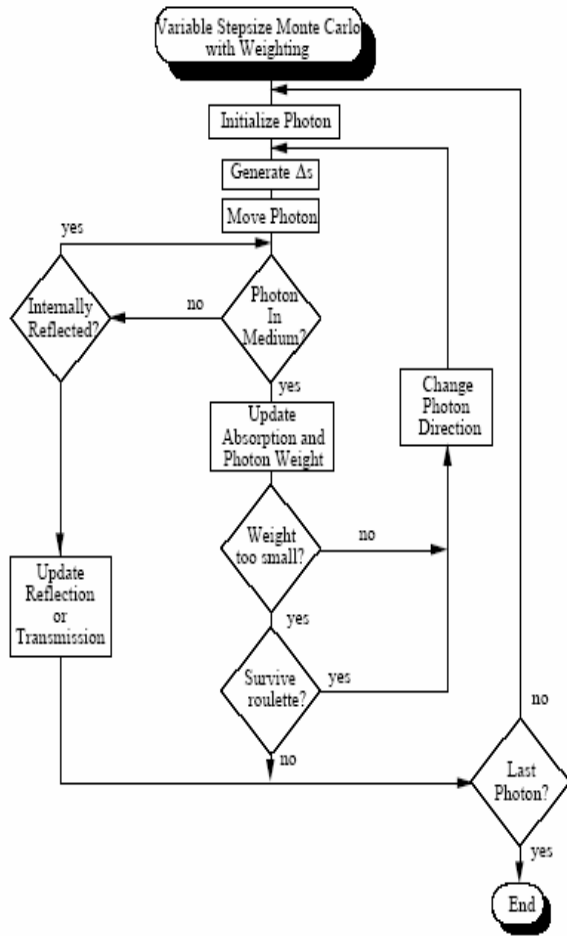


Fig. 1 Flowchart for the Monte Carlo technique [5].

### 3 Modeling heat transport in biological tissue

Heat transport is achieved through four different pathways: conduction, convection, evaporation, and radiation [9]. The standard form of heat transport equation in biological tissue is depicted below, where heat generation from metabolic activities of live tissue is neglected [10, 11, 12].

$$\rho c \frac{\partial T}{\partial t} = \nabla(\lambda \nabla T) + \rho_b c_b w_b [T_a - T] + q \quad (1)$$

Parameters used in the above equation are introduced in table 1. In homogeneous tissues with asymmetric structures, heat transport equation can be solved based on cylindrical coordinates [13]. One of these techniques is finite difference, which is based on the quantization of time and position space, based on physical parameters of the problem. Another technique is finite element which uses weighted integration. Compared with these two techniques, the finite volume technique has shown to be more successful as it covers the concept of conservation in its quantization procedure. In solving heat transport problems for example, energy

conservation dominates the quantization requirements. For this purpose, integration is done for a single timing step  $\Delta t$  over a predefined control volume (figure 2).

Table 1 Meaning of parameters used in this paper.

$\rho$ [Kg.m <sup>-3</sup> ]	Tissue density
$c$ [J.Kg <sup>-1</sup> .K <sup>-1</sup> ]	Tissue specific heat
$\lambda$ [W.m <sup>-1</sup> .K <sup>-1</sup> ]	Tissue conductivity
$\rho_b$ [Kg.m <sup>-3</sup> ]	Blood density
$c_b$ [J.Kg <sup>-1</sup> .K <sup>-1</sup> ]	Blood specific heat
$w_b$ [s <sup>-1</sup> ]	Blood flux in cubic meter
$T_a$ [K]	Arterial blood temperature
$T_v$ [K]	Venus blood temperature
$q$ [W.m <sup>-3</sup> ]	Laser fluence
$h_c$ [W.m <sup>-2</sup> .K <sup>-1</sup> ]	Thermal conductivity
$T_e$ [K]	Ambient temperature
$\sigma$ [W.m <sup>-2</sup> .K <sup>-4</sup> ]	Stefan- Boltzman constant
$\epsilon$	Emissivity
$h_{fg}$ [J.Kg <sup>-1</sup> ]	Phase transient enthalpy
$T_s$ [K]	Temperature in superficial layers
$h_m$ [m.s <sup>-1</sup> ]	Mass transport coefficient
$\rho_{v,c}$ [Kg.m <sup>-3</sup> ]	Water vapor density in air
$\rho_{v,sat}$ [Kg.m <sup>-3</sup> ]	Saturated vapor density in superficial temperature

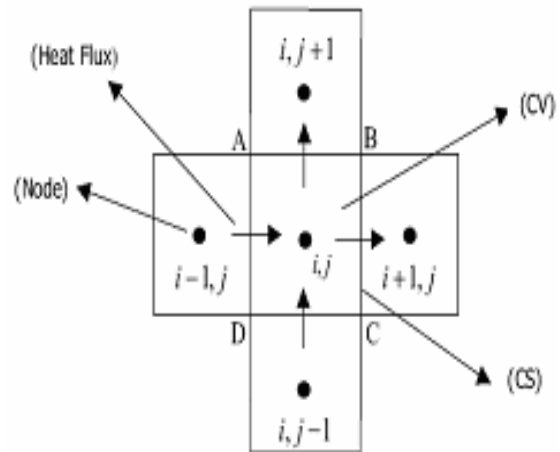


Fig. 2 Tissue segmentation in implicit finite volume.  $i, j$  show the nodal points.

By applying Gaussian divergence theory the following equation, which describes the basis of quantization in finite volume method, will result.

$$\int_{\Delta t} \frac{\partial}{\partial t} \left( \int_{CV} \rho C T dV \right) dt = \int_{\Delta t} \int_A n \cdot (\lambda \nabla T) dA dt + \int_{\Delta t} \int_{CV} \rho_b c_b w_b [T_a - T] dV dt + \int_{\Delta t} \int_{CV} q dV dt \quad (2)$$

In equation (2) CV, A and  $n$  represent control volume, surface and the vector perpendicular to the control surface.

The physical explanation of equation (2) lies in the principle of energy conservation in the control volume. For the control volume (ABCD), equation (2) can easily be quantized for heat flux using finite difference

estimation techniques. By assuming  $C$ ,  $\rho$  and  $\lambda$  as constant values and also neglecting blood circulation in the tissue, the quantization is accomplished by either explicit or implicit strategies.

The weakness of explicit methods is that they have limited stability regions because of their strong sensitivity to the timing steps. In contrast, implicit methods have extensive stability regions and therefore are more practical. In these techniques, the quantized equation for every control volume includes the unknown quantities of temperature in adjacent nodes for the timing order of  $n+1$ . Solving the linear equation system provides us with the nodes temperature. In these methods time is also involved in the quantization process. Here, it is going to be demonstrated that the steady state response is attained with less computational time. Equation (3) gives the quantization result as follows:

$$\left(\frac{\rho C}{\Delta t} + \frac{2\lambda}{\Delta r^2} + \frac{2\lambda}{\Delta z^2}\right)T_{i,j}^{n+1} - \frac{\lambda}{\Delta r^2}T_{i+1,j}^{n+1} - \frac{\lambda}{\Delta z^2}T_{i,j+1}^{n+1} - \frac{\lambda}{\Delta r^2}T_{i-1,j}^{n+1} - \frac{\lambda}{\Delta z^2}T_{i,j-1}^{n+1} = \frac{\rho C}{\Delta t}T_{i,j}^n + q_{i,j} \quad (3)$$

where  $n$  and  $n+1$  represent old and new timing steps.  $i$  and  $j$  are depth and radius indices. In order to solve equation (3),  $i$  and  $j$  are presupposed to be as follow:

$$2 \leq j \leq N_z - 1, \quad 2 \leq i \leq N_r - 1$$

where  $N_r$  and  $N_z$  are the number of divided sections in depth and radius. Other parameters are introduced in table 1. In case of two dimensional space, no thermal energy passes the central axis, because of the radial symmetric structure of the tissue, and it is also assumed that lateral and lower surfaces are far from the irradiance center. Therefore boundary conditions can be defined as follow [14]:

$$a \frac{\partial T}{\partial r} \Big|_{r=0} = \frac{\partial T}{\partial r} \Big|_{r=r_{\max}} = \frac{\partial T}{\partial z} \Big|_{z=z_{\max}} = 0 \quad (4)$$

and for the pinnacle surface of tissue we have:

$$-\lambda \frac{\partial T_s}{\partial z} = h_c(T_c - T_s) + \sigma \varepsilon(T_c^4 - T_s^4) + h_{fg}h_m(\rho_{v,e} - \rho_{v,sat}) \quad (5)$$

All constant and parameters used in equation (5) are delineated in table 1.

#### 4 Simulation results

Thermal effects of laser in two biological tissues namely those of dog and human prostates have been investigated, assuming a diode laser pulse with a wavelength of 850nm being applied to a single layered tissue as illustrated in figure 3. It needs to be mentioned that laser beam is assumed to be monotonous and its diameter is about 1mm.

Optical and thermal characteristics of dog and human prostate tissues are presented in tables 2.

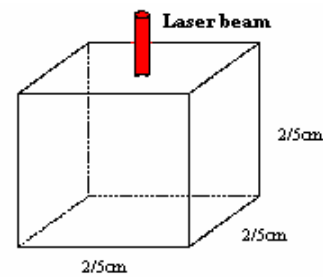


Fig. 3 Tissue and laser beam in contact surgery.

Table 2 Optical and thermal parameters of dog prostate tissue for diode laser (850nm) [15, 16].

	Dog prostate tissue	Human prostate tissue
$\mu_a$ [ $\text{cm}^{-1}$ ]	0.55	0.6
$\mu_s$ [ $\text{cm}^{-1}$ ]	120	100
$g$	0.96	0.94
$n$	1.33	1.33
$C$ [ $\text{Jkg}^{-1}\text{k}^{-1}$ ]	3662	3662
$\rho$ [ $\text{kgm}^{-3}$ ]	1060	1060
$\lambda$ [ $\text{wm}^{-1}\text{k}^{-1}$ ]	0.512	0.512
$T_i$ [ $^{\circ}\text{C}$ ]	20	37

All simulations have been done in MATLAB, where laser power and exposure time have been chosen to be 4.6W and 20min respectively. All the results, illustrated in the proceeding paragraphs, are derived from the simulation procedure. In order to have a realistic comparison between results obtained here and those derived from clinical experiments, test points depth is presumed to be 12.5mm, like those in clinical experiments [17]. Their radial distances from the laser beam position are also 5mm and 10mm. In figures 4-A and 4-B photon density distribution is plotted versus tissue radius and depth for dog prostate. In figure 5 (A and B) the tissue temperature changes obtained from simulation are illustrated along with the experimental results. The strong similarities between these two figures confirm our simulation validity. The final temperatures of selected test points, derived from the last timing step, are presented in figure 6.

One of the dominant parameters in solving equation (3) is  $\Delta t$ , the timing step, which determines the stability criterion. One of the major advantages of implicit finite volume technique is its robustness to the length of timing steps. As illustrated in figure 7, this technique allows the determination of fairly accurate response after a single timing step. Here different step widths are chosen to evaluate the thermal response. Our results have shown that thermal response with timing steps  $\Delta t=1\text{sec}$  and  $\Delta t=0.1\text{sec}$  are pretty alike, even after a single step (figure 8). Finally in figure 9 thermal response in different steps is represented in a specific test point. It can easily be comprehended that by using this method satisfactory temperature distribution in the target tissue can be determined in only a single step. The validity of the outcome of this section of simulation can

be confirmed through a brief comparison with those obtained from experiments (figure 5-a).

### 5 Conclusion

In this research, thermal interaction of laser with biological tissue was explored, using implicit finite volume method. By comparing experimental and calculated results it was demonstrated that this technique provides a reliable tool for predicting the

outcome of certain clinical experiments. The last step of our simulation revealed the robustness of this method, as valid results has been obtained in a single timing step. Consequently it is concluded that the proposed method provides strong means for simulating thermal distribution of absorbed light in tissue having the main advantages of reducing the complexity and computation time of the calculations yet maintaining a good level of accuracy and validity.

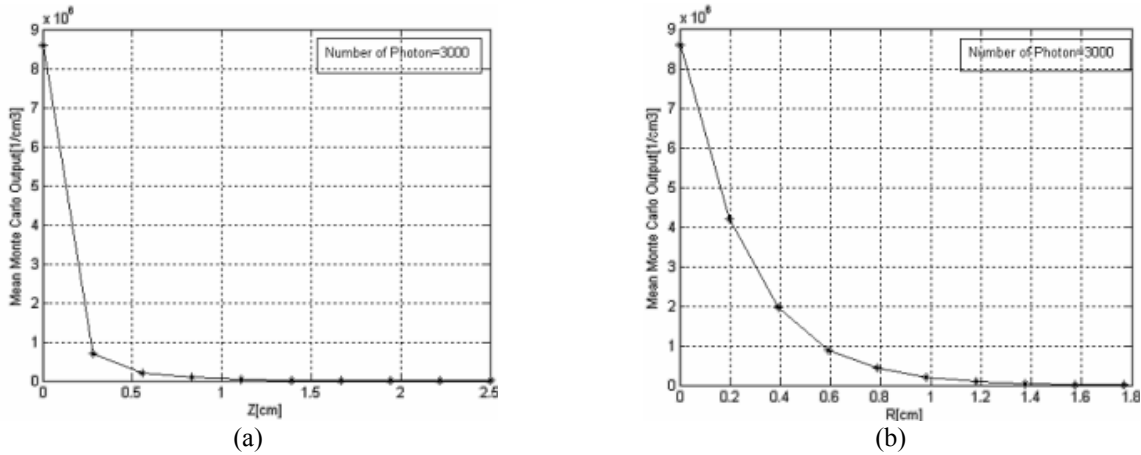


Fig. 4 Photon density in dog prostate tissue while applying diode laser. (a) axial distribution (b) radial distribution.

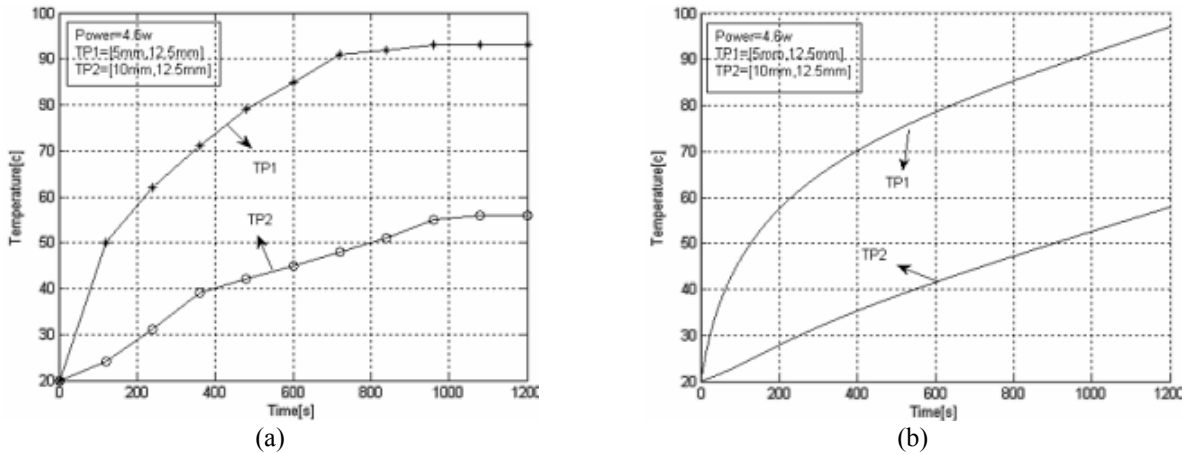


Fig. 5 Temperature changes in dog prostate tissue irradiated with a diode laser. (a) Derived from clinical experiments [17] (b) Simulation results.

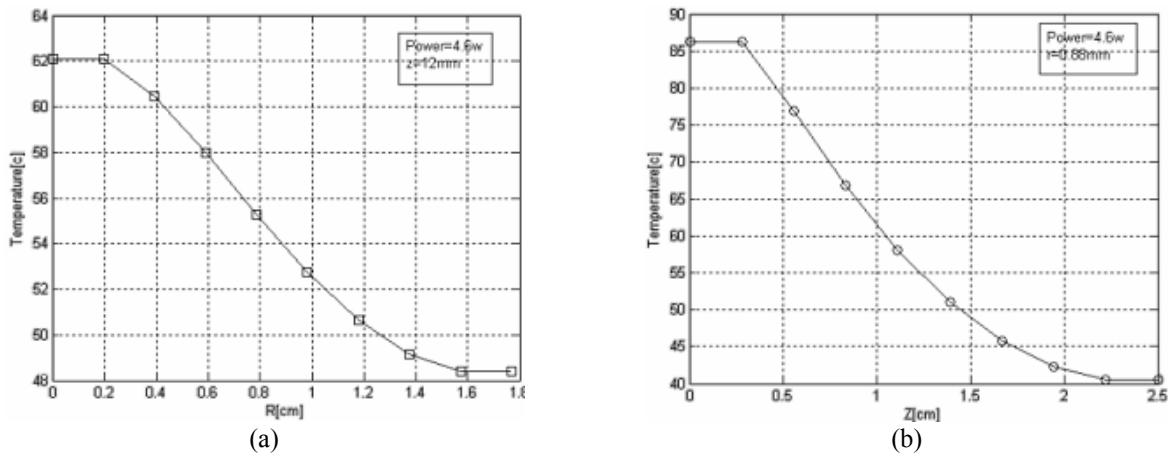


Fig. 6 Temperature changes in dog prostate tissue while applying diode laser. (a) axial distribution (b) radial distribution.

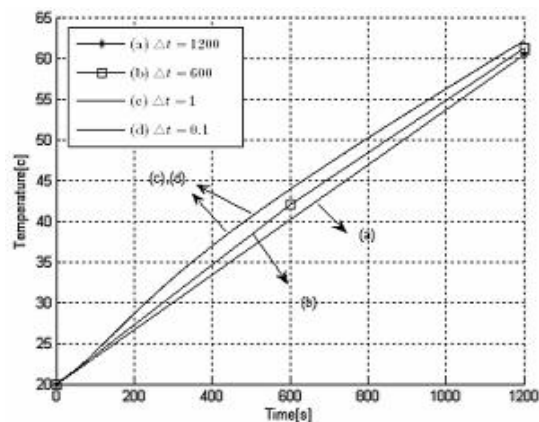


Fig. 7 Temperature changes of dog prostate tissue with different timing steps.

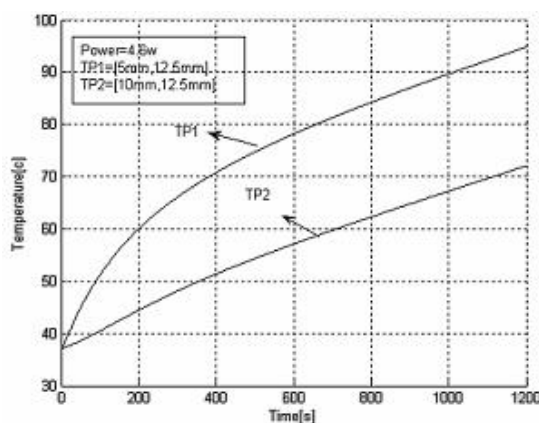


Fig. 8 Temperature changes of human prostate tissue with a single timing step.

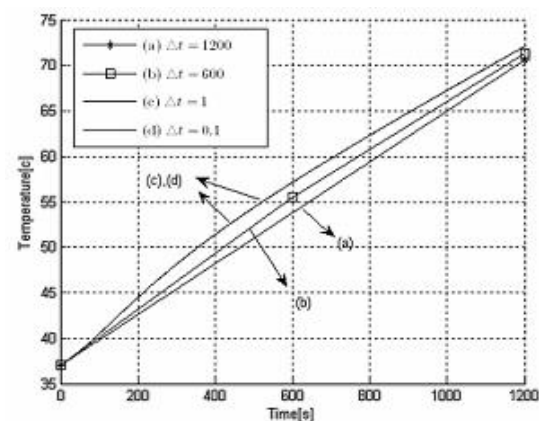


Fig. 9 Temperature changes of human dog prostate tissue with different timing steps.

## References

- [1] M. H. Niemz, *Laser-Tissue Interaction: Fundamentals and Applications*. Berlin, Heidelberg: Springer-verlag, 1996.
- [2] H. K. Versteeg and W. Malalasekera, *An Introduction to Computational Fluid Dynamics: Finite Volume Method*. Englewood cliffs, NJ, USA: Prentice Hall, 1996.
- [3] S. V. Patankar, *Numerical Heat Transfer and Fluid Flow*. Hemisphere Publishing Corporation, Newyork: 1980.
- [4] D. A. Anderson, J. C. Tannehill and R. H. Pletcher, *Computational Fluid Mechanics and Heat Transfer*. Hemisphere Publishing Corporation, Newyork: 1984.
- [5] S. L. Jacques and L. Wang, "Monte Carlo Modeling of Light Transport in Multi-Layered Tissue in Standard C", *Oregon Medical Laser Cancer*, 1998.
- [6] S. A. Prahl, *Light Transport in Tissue*, Ph.D. Thesis in the University of Texas at Austin, 1988.
- [7] V. G. Kolinko, F. F. M. De Mul, J. Greve and A. V. Priezzhev, "On Refraction in Monte Carlo Simulations of Light Transport Through Biological Tissues", *Med. Biol. Eng. Comp.*, Vol. 35, pp. 287-288, 1997.
- [8] L. Wang and S. L. Jacques, "MCML\_Monte Carlo Modeling of Light Transport in Multi-Layered Tissues", *Comput. Methods Prog. Biomed.*, Vol. 47, pp. 131-146, 1995
- [9] J. P. Holman, *Heat Transfer*. MC Graw Hill: 1981.
- [10] R. Anderson and A. Rox, "Thermal Properties of Tissue", *Tissue Optics Course*, 2002.
- [11] J. W. Valvano, "Bioheat Transfers", *Biomedical Engineering Program Department of Electrical and computer Engineering*, The university of Texas at Austin, pp. 1-46.
- [12] M. A. Trelles, *Heat Conduction*. John Willy Edition: 1987, Chapter Six.
- [13] C. Sturesson and S. Anderson-Engels, "A Mathematical Model for Predicting the Temperature Distribution in Laser-Induced Hyperthermia : Experimental Evaluation and Applications", *Phys. Med. Boil.*, Vol. 40, pp. 2037-2052, 1995
- [14] J. Heisterkamp, R. V. Hillegersberg and J. N. M. IJ Zermans, "Critical Temperature and Heating Time for Laser Coagulation (ILC) of Tumors", *Laser in Surgery and Medicine*, Vol. 25, pp. 257-262, 1999.
- [15] C. T. Germer, A. Roggan, J. P. Ritz, C. Isbert, D. Albercht, G. Muller and H. J. Buhr, *Optical properties of native and coagulated human liver tissue and liver metastases in the near infrared range*, *Laser in Surgery and Medicine*, Vol. 23, pp. 194-203, 1998.
- [16] L. C. L. Chin, W. M. Whelan and I. A. vitkin, "Models and Measurements of Light Intensity changed during laser interstitial thermal therapy: Implications for Optical Monitoring of the

Coagulation Boundary Location”, *Phys. Med. Bio.*, Vol. 48, pp. 243-559, 2003.

[17] V. Prapavat, A. Roggan, J. Walter, J. Beuthan, U. Klingbeil and G. Muller, “In vitro Studies and

Computer Simulation to Assess the Use of a Diode Laser (850nm) for Laser-Induced Thermotherapy (LITT)”, *Laser in surgery and Medicine*, Vol. 18, pp. 22-33, 1996.